AB

KEK Preprint 93-174
AMY 93-4
December 1993
H

Measurement of the Inclusive Jet Cross Section in Photon-Photon Interactions at TRISTAN

The AMY Collaboration

Submitted to Phys. Lett.

National Laboratory for High Energy Physics, 1993

KEK Reports are available from:

Technical Information & Library
National Laboratory for High Energy Physics
1-1 Oho, Tsukuba-shi
Ibaraki-ken, 305
JAPAN

Phone: 0298-64-1171
Telex: 3652-534 (Domestic)
(0)3652-534 (International)
Fax: 0298-64-4604
Cable: KEK OHO
E-mail: LIBRARY@JPNKEKVX (Bitnet Address)
library@kekvax.kek.jp (Internet Address)

Measurements of the inclusive jet cross section in photon-photon interactions at TRISTAN

The AMY Collaboration

B.J.Kim [a], T.Nozaki [b], A. Bodek [a], T.Kumita [a], Y.K. Li [a], C.Velisarris [a], R.C.Walker [a], K.Abe [b], R.E.Breedon [b,h], Y.Fujii [b], Y.Kurihara [b], F.Liu [b], A.Maki [b], T.Omori [b], H.Sagawa [b], Y.Sakai[b], T.Sasaki [b], Y.Sugimoto [b], Y.Takaiwa [b], S.Terada [b], P.Kirk [c], C.P.Cheng [d], W.X.Gao [d], W.G.Yan [d], M.H.Ye [d], A.Abashian [e], K.Gotow [e], D.Haim [e], M.E.Mattson [e], N.Morgan [e], L.Piilonen[e], K.L.Sterner [e], S.Lusin [f], C.Rosenfeld [f], S.Wilson [f], L.Y.Zheng [f], C.A.Fry [g], R.Tanaka [g],L.M.Chinitz [h], Winston Ko [h], R.L.Lander [h], J.Rowe [i], J.R.Smith [h], D.Stuart [h], S.Kanda [i], S.L.Olsen [i], K.Ueno [i], F.Kajino [j], T.Thomas[k], T.Aso [l], K.Miyano [l], H.Miyata [l], K.Ohkubo [l], M.Oyoshi [l], M.Shirai [l], Y.Yamashita [m], M.H.Lee [n], F.Sannes [n], S.Schnetzer [n], R.Stone [n], J.Vinson [n], S.Behari [o], S.Kobayashi [o], A.Murakami [o], S.K.Sahu [o], Y.S.Chung [p], D.K.Cho [p], J.S.Kang [p], D.Y.Kim [p], K.B.Lee [p], K.W.Park [p], S.K.Kim [q], S.S.Myung [q], S.K.Choi [r], D.Son [r], S.Ebara [s], S.Matsumoto [s], N.Takashimizu [s], and T.Ishizuka [t]

[a] *University of Rochester, Rochester, NY 14627, USA*
[b] *KEK, National Laboratory for High Energy Physics, Ibaraki 305, Japan*
[c] *Louisiana State University,Baton Rouge,LA 70803, USA*
[d] *Institute of High Energy Physics, Beijing 100039, China*
[e] *Virginia Polytechnic Institute and State University, Blacksburg,VA 24061, USA*
[f] *University of South Carolina, Columbia, SC 29208, USA*
[g] *SSC Laboratory, Dallas, TX 75237, USA*
[h] *University of California, Davis, CA 95616, USA*
[i] *University of Hawaii, Honolulu, HI 96822, USA*
[j] *Konan University, Kobe 658, Japan*
[k] *University of Minnesota, Minneapolis, MN 55455, USA*
[l] *Niigata University, Niigata 950-21, Japan*
[m] *Nihon Dental College, Niigata 951, Japan*
[n] *Rutgers University, Piscataway, NJ 08854, USA*
[o] *Saga University, Saga 840, Japan*
[p] *Korea University, Seoul 136-701, South Korea*
[q] *Seoul National University, Seoul 151-742, South Korea*
[r] *Kyungpook National University, Taegu 702-701, South Korea*
[s] *Chuo University, Tokyo 112, Japan*
[t] *Saitama University, Urawa 338, Japan*

We present cross section measurements for inclusive jet production in almost-real photon-photon interactions at TRISTAN using the AMY detector. The results are compared with leading-order QCD calculations for different parameterizations of the parton density in the photon.

1. Introduction

Resolved photon processes in $\gamma\gamma$ collisions are hard, non-diffractive hadronic interactions in which a constituent parton in one of the photons interacts with the other photon or one of its constituents. In such processes, the interacting constituents produce wide-angle jets and the noninteracting constituents produce spectator jets in the directions of the incident photons. Hadron-jet production via resolved photon processes in high energy real $\gamma\gamma$ collisions was first discussed in 1978-1979 by Brodsky *et al.* [1] and Kajantie and Raito [2]. The possibility of using measurements of resolved photon processes at existing accelerators to determine the parton densities in the photon was pointed out recently by Drees and Godbole [3].

While data from PEP and PETRA experiments show some indications of resolved photon processes [4, 5], their existence was first conclusively demonstrated by the AMY group at TRISTAN [6]. Subsequently, the H1 and ZEUS experiments reported observations of resolved photon processes in γp collisions at the HERA ep collider[7, 8]. Recently the TOPAZ group at TRISTAN [9] and the ALEPH group at LEP [10] have also observed resolved photon processes. Resolved photon processes are expected to be the dominant source of high-p_T hadron production in very high energy e^+e^- collisions and have been identified as a potentially serious background for experiments at future linear colliders [11]. Precise measurements of resolved photon processes at existing energies will help provide realistic estimates of these background levels.

We report on an experimental study of jet production in high energy $\gamma\gamma$ collisions. The experiment uses reactions of the type $e^+e^- \to e^+e^- + hadrons$ at $E_{cm} \simeq 60$ GeV, where both the electron and positron scatter at small angles (untagged events) and the virtual photons are nearly on the mass shell.

The experimental results reported here are based on a 27.2 pb^{-1} data sample accumulated in the upgraded AMY detector (AMY-1.5) at the TRISTAN e^+e^-storage ring. Results based on a 27.5 pb^{-1} data sample taken by the original AMY detector

(AMY-1.0) have already been published [6]. The AMY-1.5 detector has improved coverage in the forward-backward angular regions. In addition, the current analysis uses a Monte Carlo calculation of the resolved photon processes (MJET) that has been improved to include the effects of

- the finite mass of the charm quark,
- the finite intrinsic p_T of the spectator jet, and
- string fragmentation of quarks and partons [12].*

In ref. 6, we reported the results of a thrust analysis in the center of mass system of the detected hadrons in which hadrons from the spectator jets were included. The events were each divided into two hemispheres defined by the plane perpendicular to the thrust axis, the particles in each hemisphere were combined and treated as a jet; the component of the jet momentum relative to the beam direction was denoted as P_T^{jet}. The observed thrust and P_T^{jet} distributions clearly indicate that it is necessary to include contributions from resolved photon processes to reproduce the data. In the present analysis, we identify jet-like particle configurations produced by hard-scattering processes and evaluate inclusive jet cross sections in almost-real $\gamma\gamma$ collisions. A similar analysis was done by the TOPAZ group [9]. There are two advantages of the present analysis over the previous one: the results do not suffer from any ambiguity in the simulation of the spectator jets, such as the unknown value of the intrinsic p_T of the spectator jet; and the jet cross sections have a clear correspondence to parton-level cross sections, which can be directly compared to theory.

2. Event selection

Selection of untagged $\gamma\gamma \to hadrons$ events

*In our previous paper [6] we stated that the string fragmentation scheme was used. We recently found that the calculations reported in this paper used, in fact, the independent fragmentation scheme.

In the 1989 upgrade, the two separate endcap shower counters (PTC, RSC) of AMY-1.0 were replaced by the single shower counter (ESC) of AMY-1.5. This upgrade provided a more uniform coverage for photons and electrons and extended the angular acceptance to $\theta \geq 13^0$. The details of the AMY detector have been reported elsewhere [13].

Untagged hadronic events produced by $\gamma\gamma$ interactions are selected by the following requirements:

- a minimum of four charged tracks with polar angles in the range $25° \leq \theta \leq 155°$, of which at least two must have $|p| > 0.75$ GeV/c and at least one must have $p_t > 1.0$ GeV/c;
- the most energetic cluster appearing in the calorimeter, covering $|\ cos\theta\ | \leq 0.97$, must have an energy less than $0.25E_{beam}$ (anti-tagging);
- the net charge of the observed charged tracks $\sum q_i \leq 2$;
- the net transverse momentum is limited to $|\sum \vec{p}_{t,i}| \leq 5.0$ GeV/c, where $\vec{p}_{t,i}$ are the projections of the observed momenta on the plane transverse to the beam; and
- the invariant mass of observed hadrons must be in the range 4 GeV/c$^2 \leq W_{vis} \leq$ 20 GeV/c^2, where the calculation of W_{vis} includes both charged and neutral particles and a pion mass is assigned to all charged particles.

The 3248 events that survived these cuts were visually scanned by physicists. In the scan, 451 events were attributed to stray beam particles interacting in the wall of the vacuum chamber and were discarded.

Hadronic annihilation events with either initial state radiation or a large amount of missing energy can satisfy the $e^+e^- \to e^+e^- + hadrons$ selection criteria. The level of this contamination was estimated using an event sample generated by the Lund

6.3 event generator[14], which was passed through a detector simulation program. The contamination from $e^+e^- \to \tau^+\tau^-$ and $e^+e^- \to e^+e^-\tau^+\tau^-$ was also estimated by using Monte Carlo simulated events for these processes. The background estimates we obtain are

- hadronic annihilation: 73 ± 6 events;
- $e^+e^- \to e^+e^-\tau^+\tau^-$: 66 ± 6 events; and
- $e^+e^- \to \tau^+\tau^-$: negligibly small.

From the distribution of vertex positions along the beam line we conclude that the residual contamination from beam-gas events is negligibly small.

The trigger efficiency for $e^+e^- \to e^+e^- + hadrons$ events that satisfy the selection criteria was estimated using a Monte Carlo simulation to be 97.1 ± 1.8%. After all background subtraction and efficiency corrections, we obtain a final count of 2738 ± 76 events. The stated error is the quadrature sum of the statistical errors (1.9%) and the systematic uncertainties of the luminosity measurement (1.8%), trigger efficiency (1.6%), and scanning efficiency (2%).

Jet selection

In order to find jets in the data sample selected as above, we apply the cone-algorithm that is widely used in the analysis of hadron-hadron collisions and is implemented, for example, in the LUCELL program in JETSET 7.3 [12]. Following the jet definition given in ref.15, all particles within a cone of radius $R = 1$ in pseudo-rapidity η and azimuth ϕ space [†] are combined. The transverse momentum of the jet relative to the e^+e^- beamline, P_T^{jet}, is the sum of the transverse momenta of the particles within the cone. Initially, the highest p_t particle is used to define the axis of the jet. Subsequently, the jet axis, (η^{jet},ϕ^{jet}), is determined by averaging the η and ϕ values of the individual

[†] $R \equiv \sqrt{\Delta\eta^2 + \Delta\phi^2}$

particles weighted by their transverse momenta. The resulting jet axis is used to define a new jet cone and this procedure is iterated until the jet cone remains unchanged. Such a jet search is repeated until no further jets are found. Two adjacent jets are combined into one jet if both jet axes are inside the $R = 1$ cone of the combined jet. We only accept jets with two or more particles and with $P_T^{jet} > 2.5$ GeV/c and $|\eta^{jet}| < 1.0$. The $P_T^{jet} > 2.5$ GeV/c cut minimizes the Generalized Vector Meson Dominance model(GVMD) [16] contribution and thus reduces the effect of the choice of P_T^{min}. The $|\eta^{jet}| < 1.0$ cut restricts the jet axes to directions that are well contained in the detector acceptance, where charged (neutral) particles with $|\eta| < 1.5$ (2.2) are detected with uniform efficiency. We found a total of 1392 jets; 254 events have two jets, and no event has three or more jets.

The background contamination for inclusive jets (two-jet events), evaluated from the Monte Carlo background events mentioned above, are

- hadronic annihilation: 63.8 ± 5.3 jets (11.5 ± 1.6 events);
- $e^+e^- \to e^+e^-\tau^+\tau^-$: 56 ± 5.4 jets (8 ± 1.4 events); and
- $e^+e^- \to \tau^+\tau^-$: negligibly small.

3. Monte Carlo simulations

The experimental data are compared with the predictions of models for jet production in $\gamma\gamma$ reactions using Monte Carlo simulations. Point-like interactions of photons are modeled using a quark-parton model (QPM) event generator that incorporates all first-order QED radiative corrections [17]. The final-state quarks in the QPM events are fragmented via the Lund parton-shower scheme using the default parameters.[‡] Diffractively produced hadrons are modeled using the Generalized Vector Meson Dominance model (GVMD) [16]. A sample of simulated GVMD events were produced using the techniques developed by the PLUTO group [18, 5]. Here a $\gamma\gamma$ total cross section of

[‡] In the previous study[6], the LUND string fragmentation scheme was used for the QPM.

$\sigma_{\gamma\gamma}$=240 nb is used and the produced final state is treated as a massive quark-antiquark system that is subsequently converted to hadrons via the Field-Feynman fragmentation scheme [19]. We use the PLUTO-tuned parameters and, like the PLUTO group, limit the p_T distribution by an exp(-5p_T^2) factor.

To simulate resolved photon processes, we have developed the MJET event generator[6] based on the BASES and SPRING programs by Kawabata [20]. MJET generates events according to the formulae given in ref. 3, using various parametrizations for the parton densities in the photon. The cross section formulae for the subprocesses involving final-state $c-$quarks have been modified to include its mass, which is taken to be 1.6 GeV/c^2. The number of flavors in photon are switched from three to four depending on the hardness of the subprocesses involved.[§]

The MJET cross section for three- (four-) jet events is given by the product of the luminosity functions of two photons [21]; the parton density inside one photon (parton densities inside two photons); the subprocess cross section for the interaction between a parton and a photon (between two partons); and a kinematic factor. The subprocess cross sections have been calculated by perturbative-QCD [22]. The MJET simulations are carried out by producing two high-P_T partons and one (two) spectator parton(s) corresponding to three- (four-) jet events. The produced partons are hadronized by the Lund string-fragmentation scheme, using the Lund 6.2 program's default values for the fragmentation parameters [23].

Spectator jets are simulated by generating a parton with finite transverse momentum with respect to the incident beam direction, $P_{T,spec}$. Here, the $P_{T,spec}$ distribution is taken to be proportional to $1/(P_{T,spec}^2 + P_{T,spec,0}^2)$ with $P_{T,spec,0}$ = 0.4 GeV/c. Values of $P_{T,spec,0}$ of this order of magnitude eliminate the divergence in the distribution with little effect on the observed distributions.

We use parton density parameterizations given by Drees and Godbole (DG) [24],

[§]In our previous analysis[6], we treated all quarks as massless and the number of flavors was taken to be four.

Levy, Abramowics and Charcula, (LAC) [25], and Gluck, Reya and Vogt (GRV) [26]. Both the DG and LAC parton density parameterizations are obtained by solving the leading-order Q^2 evolution equation. The GRV densities are obtained from a leading-order QCD evolution with the assumption that the parton density at Q^2 = 0.25 (GeV/c)^2 is given by GVMD. The Q^2 evolution of the DG parameterization starts from Q_0^2=1 (GeV/c)^2 and parameters are fitted to the PLUTO F_2^γ structure function data at Q^2 =5.9 (GeV/c)^2 by imposing reasonable relations among the singlet quark, non-singlet quark, and gluon densities [24]. For the DG density, we include $c\bar{c}$ production for those events where the parton P_T exceeds 7 GeV/c. The LAC parameterizations are obtained by fitting parameters to all available F_2^γ experimental data from Q^2 = 1 to 100 (GeV/c)^2 without the imposition of any relationships among the parton densities [25]. For the LAC densities, we include $c\bar{c}$ production when the $\gamma\gamma$ c.m. energy exceeds 10 (GeV/c)^2. Three LAC parametrizations are available, LAC1, LAC2 and LAC3, with Q^2 evolutions starting at Q_0^2 = 4.0, 4.0, and 1.0 (GeV/c)^2, respectively.

In Fig. 1a we compare the photon structure function $F_2^\gamma(x,Q^2) = \sum e_i^2 x q_i(x,Q^2)$ predicted by the DG, LAC, and GRV models, where e_i and $q_i(x,Q^2)$ are the charge and the quark density of quark flavor i, respectively. Figure 1b shows a comparison of the gluon distributions $xG(x,Q^2)$ predicted by the DG, LAC and the GRV models. The LAC3 model gives an extraordinarily large gluon density at large x. Since the LAC1 and LAC2 are quite similar, we only consider LAC1 here.

As is apparent in Fig. 1, the differences in the quark densities for the DG, GRV, and all the LAC models are rather small, except for the small x region, $x \leq 0.05$. However, the gluon densities of the three models differ substantially. The QCD scale parameter Q^2 is chosen to be the P_T^2 value of the outgoing partons.

In order to both guarantee the applicability of QCD and avoid double counting between the soft (diffractive) and hard (non-diffractive) contributions, we only generate

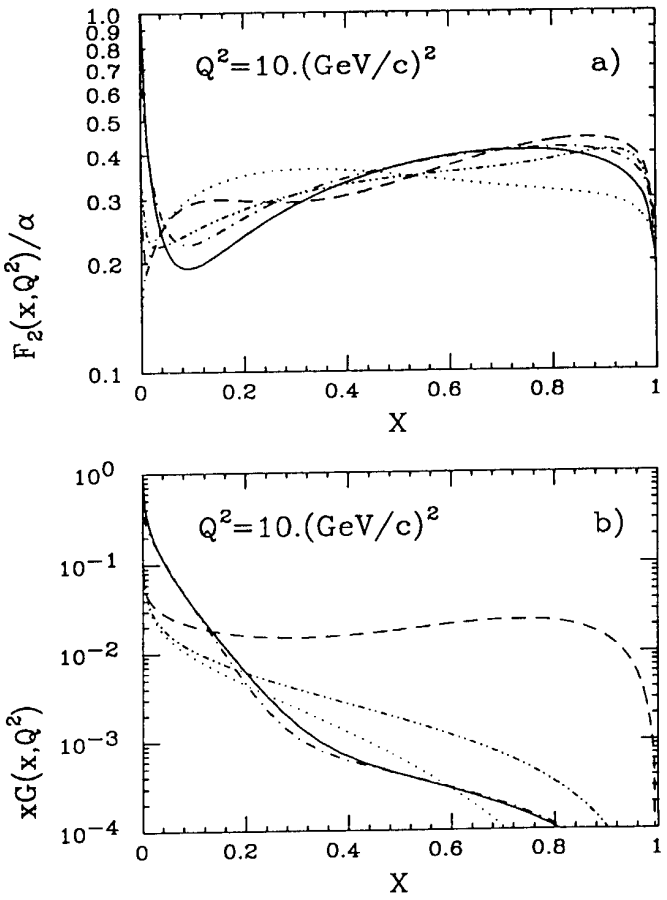

Figure 1: a) A comparison of the photon structure function $F_2^\gamma(x,Q^2)$ at Q^2 = 10 (GeV/c)^2, calculated using the LAC1, LAC2, LAC3, DG and GRV parton densities. b) A similar comparison of the gluon distribution $xG(x,Q^2)$ in the photon at Q^2 = 10 (GeV/c)^2. The solid, dot-dash, dashed, dotted and double-dot-dash curves represent the LAC1, LAC2, LAC3, DG and GRV predictions, respectively. The number of flavors is taken to be three.

events with parton P_T values larger than a cutoff P_T^{min}. Aside from the fact that the applicability of perturbative QCD requires P_T^{min} to be greater than about 1 GeV/c, the appropriate value for the cutoff is not known. Therefore, the value of P_T^{min} is treated as a free parameter and is determined from the experimental data as described below.

4. Jet analysis and Monte Carlo Comparisons

As noted above, the cone algorithm was used to find jets. For comparison purposes, the JADE clustering algorithm [27], which is widely used in the analysis of e^+e^- events, was used and found to give similar results.

The observed jet distributions were corrected by means of a bin-by-bin background subtraction and compared with Monte Carlo simulations. Fig. 2(a) shows the inclusive jet transverse momentum distribution. Also shown in the figure are the predictions for GVMD, QPM, and the sum of GVMD, QPM and MJET. Here, in the MJET model we use the LAC1 parton distributions with P_T^{min} values of 2.0, 2.2 and 2.4 GeV/c. As can be seen in the figure, the MJET contribution dominates at high transverse momentum. The GVMD contribution is only significant for P_T^{jet} values below 3 GeV/c. The inclusive P_T^{jet} data are reasonably well reproduced by the sum of GVMD, QPM and MJET with P_T^{min} = 2.2 GeV/c. In Fig. 2(b), the data are compared with the GVMD+QPM+MJET models for the LAC1 and DG parton densities. Here the P_T^{min} value for LAC1 (DG) is set to its optimized value of 2.2 (2.0) GeV/c.¶

As can be seen in the figure, the DG prediction is similar to that for LAC1 even though the gluon densities for LAC1 and DG are significantly different. We cannot, therefore, discriminate between the LAC1 and DG densities using the P_T^{jet} distribution. Fig. 3 shows transverse jet momentum distributions for inclusive two-jet events. The same conclusions obtain.

¶In our previous analysis of the thrust distribution of the AMY 1.0 data[6], we found 1.6 GeV/c as the optimum P_T^{min} value for DG.

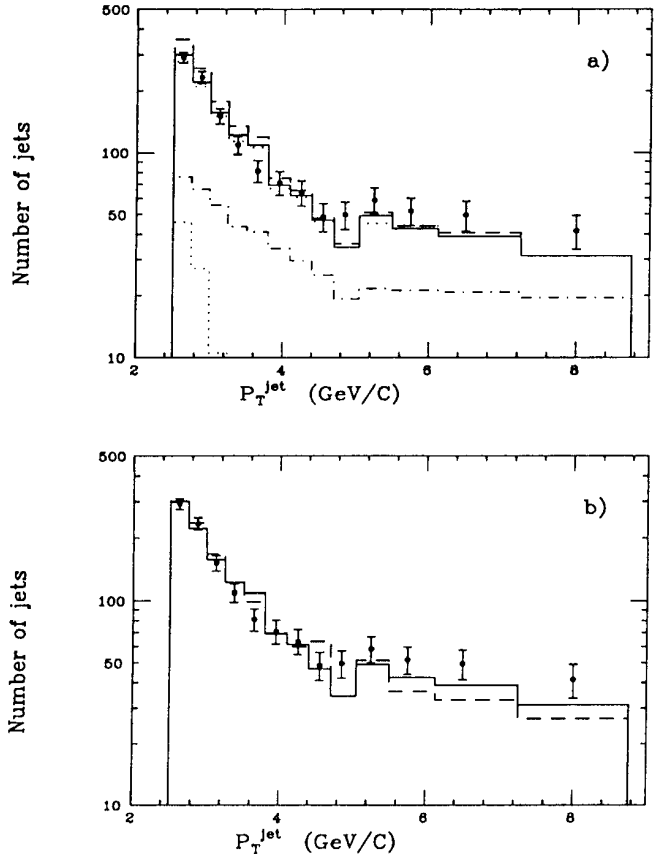

Figure 2: Comparisons of the observed transverse momentum of jets with Monte Carlo simulations. a) The histograms are the predictions of i) GVMD (lower dotted line), ii) QPM (dot-dashed line), and iii) QPM + GVMD + MJET where MJET is simulated for the LAC1 parton densities with P_T^{min} =2.0 GeV/c (dashed line), P_T^{min} =2.2 GeV/c(full line) and P_T^{min} =2.4 GeV/c (upper dotted line). In b), The histograms are the MC expectations using the LAC1 (full line) and DG (dashed line) parton densities with P_T^{min} =2.2 GeV/c and 2.0 Gev/c, respectively.

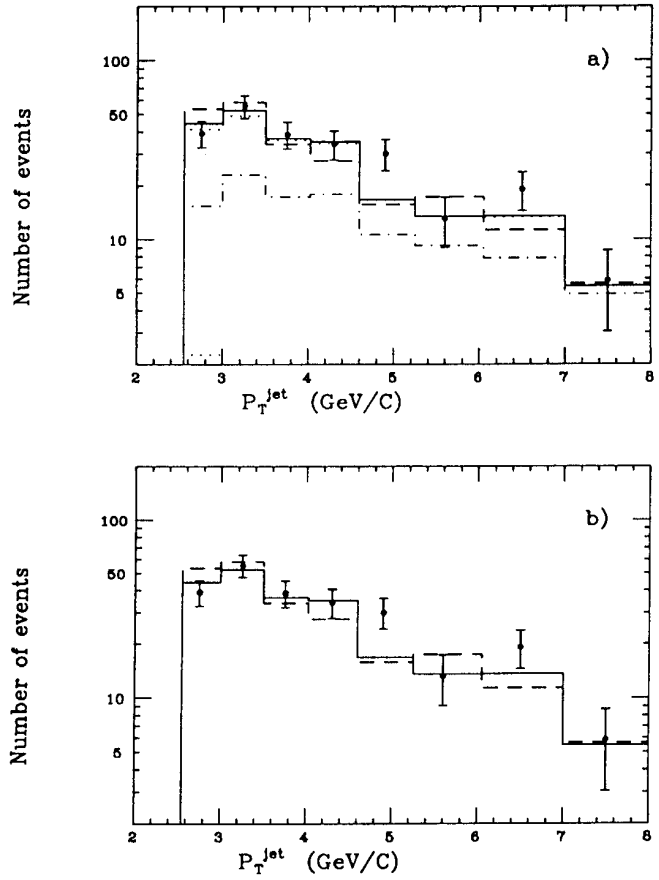

Figure 3: The same as Fig.2 for the inclusive two-jet events.

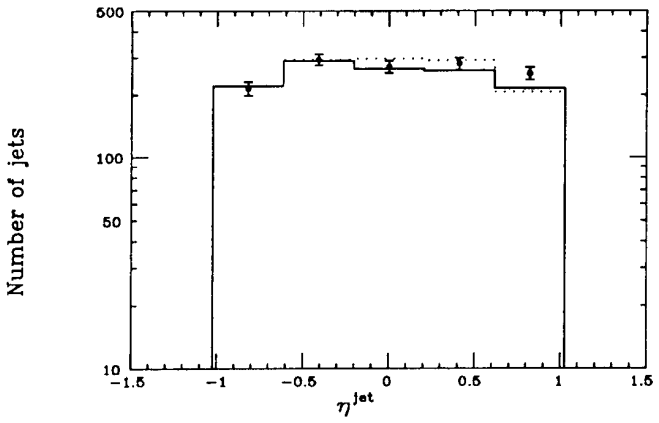

Figure 4: Comparison of the observed jet rates as a function of pseudo-rapidity with the Monte Carlo simulations(GVMD+QPM+MJET). The LAC1(full line) and the DG(dotted line) parton densities are used for the MJET Monte Carlo simulations with P_T^{min} =2.2 GeV/c and P_T^{min} 2.0 GeV/c, respectively.

We also investigated the inclusive pseudo-rapidity distribution, which is compared with GVDM+QPM+MJET models in Fig. 4. We examined the inclusive η^{jet} distribution to see if there is any distinction between the different parton density ansatzs in the MJET model. However, as in the inclusive P_T^{jet} distribution, we cannot find any clear distinction.

5. Inclusive Jet Cross Sections

In order to obtain an inclusive jet cross section for resolved photon processes, the QPM and GVMD contributions are subtracted from the observed distribution which is then corrected for detector acceptance and resolution (unfolded). The final inclusive cross sections are obtained from the sum of the unfolded cross sections and the QPM cross sections. The unfolding procedure consists of the following series of steps. (Here

the $k-th$ bin of the observed distribution for the data is denoted as $N_{data}(k)$.)

- The QPM, GVMD and the "outside-cut" MJET contributions are subtracted from the data, where the "outside-cut" contribution corresponds to MJET events with outgoing partons that fail to satisfy either $|\eta| < 1.0$ or $P_T > 2.5$ GeV/c but still produce hadron jets that are accepted.

- The acceptance, $\epsilon(i)$, for the $i-th$ bin of the P_T (or η) distribution of partons (the ratio of the number of reconstructed jets originating from the $i-th$ bin partons to the number of the $i-th$ bin partons) is determined using MJET simulations with LAC1 parton densities.

- The ratio $frac(i,k)$, the number of events where the parton's P_T (or η) is in the $i-th$ bin and the corresponding reconstructed jet P_T (or η) is in the $k-th$ bin divided by the total number of events in the $k-th$ bin of the reconstructed jet distribution, is determined using simulated MJET data.

- The $i-th$ bin of the unfolded distribution $N_{gen}(i)$ is then obtained from the expression

$$N_{gen}(i) = \sum_k frac(i,k) N_{data}(k)/\epsilon(i).$$

This unfolding algorithm is correct to the extent that the Monte Carlo simulations accurately describe the observed distributions. Since the observed $P_T^{jet}$and η^{jet} distributions are reasonably well reproduced by the GVMD+QPM+LAC1 model, this simple unfolding method should be adequate. According to the Monte Carlo simulation, the P_T^{jet} resolution varies from 1 to 2 GeV/c as P_T^{jet} increases from 2.5 to 9 GeV/c and the η^{jet} resolution is found to be 0.4 over the entire η^{jet} region.

The resulting inclusive jet and two-jet cross sections for jets with $|\eta| < 1.0$ are shown as a function of P_T in Figs. 5 and 6, respectively. The values are given in Tables 1

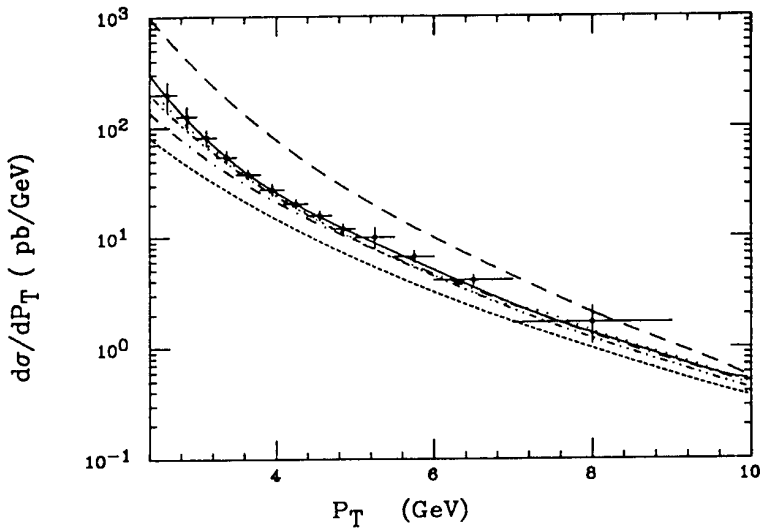

Figure 5: Inclusive jet cross section as a function of P_T integrated over $|\eta| < 1.0$. The curves represent the sum of the QPM (direct) and MJET (resolved) cross sections using the LAC1 (full line), GRV (double-dot-dashed line), DG (dotted line), LAC3 (dashed line), and LAC1 with the gluon components excluded (dot-dashed line) parton densities. The short-dashed curve represents the QPM cross section. The plotted errors are the quadrature sum of the statistical and systematic errors.

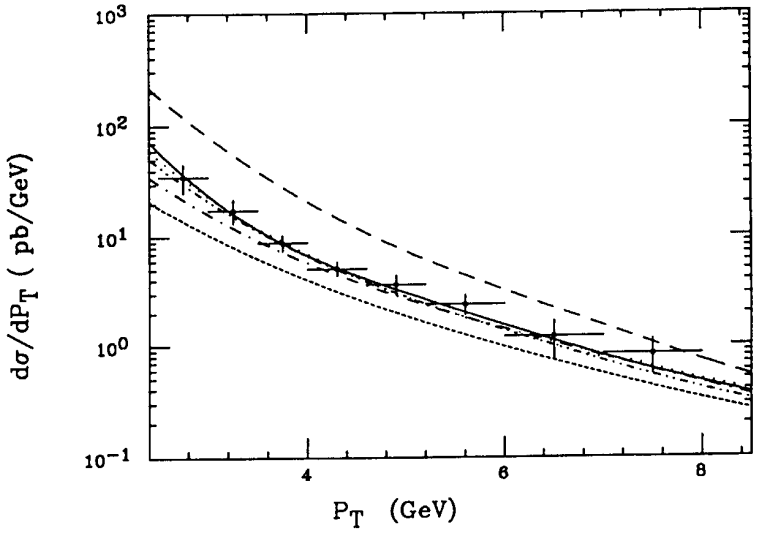

Figure 6: Same as Fig.5 for the inclusive two-jet cross section.

Table 1: Inclusive jet cross-section in the region $|\eta| < 1.0$. The statistical error and the systematic error have been added in quadrature to give the total p_T-dependent error.

p_T (GeV)	$d\sigma/dp_T$ (pb/GeV)	$\Delta(d\sigma/dp_T)$ (pb/GeV)		
		Statistical error	Systematic error	Total error
2.63	199.5	13.7	52.7	54.4
2.88	126.6	7.56	26.6	27.6
3.13	81.7	4.42	12.2	13.0
3.38	54.6	2.48	6.30	6.77
3.65	38.0	1.64	3.41	3.78
3.95	27.5	1.09	2.93	3.13
4.25	20.4	0.79	1.80	1.97
4.55	15.9	0.61	1.42	1.54
4.85	12.1	0.46	1.15	1.24
5.25	10.0	0.48	2.12	2.18
5.75	6.67	0.32	0.66	0.73
6.50	4.07	0.18	0.36	0.40
8.00	1.71	0.11	0.61	0.62

and 2. The quadratic sum of the statistical and systematic errors are indicated in the figures. The total errors vary from 10% to 36 % [15% to 37%] for the inclusive jet [two-jet] events. (Hereafter the bracketed numbers correspond to the results for the two-jet events.) The statistical errors range from 4 to 7% [11 to 22%]. The systematic errors include estimated uncertainties in the luminosity measurements of 1.8%, trigger efficiency of 1.6%, scanning efficiency of 2%, GVMD subtraction (which varies from 10% to 0.5% [3% to 0%] over the range $2.5 < P_T^{jet} < 8$ GeV/c) and the unfolding procedure (which varies from 35% to 2 % [33% to 6%] over the range $2.5 < P_T^{jet} < 8$ GeV/c). The estimated error due to the GVMD subtraction is the variation of the results when the value of $\sigma_{\gamma\gamma}$ is changed by 50%. The systematic error due to the unfolding procedure is the change of the unfolded cross sections when the DG parton density with P_T^{min}= 2.0 GeV/c is used—instead of the LAC1 parton density with P_T^{min}= 2.2 GeV/c—to calculate the correction functions. The difference in the results when independent fragmentation is used—instead of string fragmentation—gives an

Table 2: Inclusive two-jet cross-section in the region $|\eta| < 1.0$. The statistical error and the systematic error have been added in quadrature to give the total error.

p_T (GeV)	$d\sigma/dp_T$ (pb/GeV)	$\Delta(d\sigma/dp_T)$ (pb/GeV)		
		Statistical error	Systematic error	Total error
2.75	35.1	7.83	6.35	10.1
3.25	17.4	2.30	3.43	4.13
3.75	8.88	1.00	1.06	1.46
4.30	5.12	0.51	0.56	0.76
4.90	3.64	0.38	0.62	0.73
5.60	2.40	0.23	0.42	0.48
6.50	1.21	0.15	0.43	0.46
7.50	0.84	0.10	0.27	0.29

Table 3: Inclusive jet cross-section in the region $|p_T| \geq 2.5$ GeV/c. The statistical error and the systematic error have been added in quadrature to give the total error.

η	$d\sigma/d\eta$ (pb)	$\Delta(d\sigma/d\eta)$ (pb)		
		Statistical error	Systematic error	Total error
-0.82	72.9	6.1	11.5	13.0
-0.41	80.8	5.3	12.4	13.5
0.00	83.6	4.8	15.8	16.5
0.41	88.2	5.4	19.7	20.4
0.82	93.8	7.1	14.0	15.7

additional unfolding error of about 5%.

The inclusive jet cross section as a function of η for jets with $|P_T| \geq 2.5$ GeV/c is presented in Fig. 7 and in Table 3. The systematic errors due to the luminosity measurements, trigger efficiency, scanning efficiency and the hadronization scheme are the same as those for the inclusive jet cross section as a function of P_T^{jet}. The error due to the GVMD subtraction is about 6% for each bin of η and the errors due to the unfolding procedure range from 12% to 21%.

Since the results correspond to parton-level cross sections, we compare them directly to theoretical calculations in Figs. 5, 6, and 7. For resolved process calculations we use the parton densities in the photon given by LAC1, LAC3, DG and GRV models.

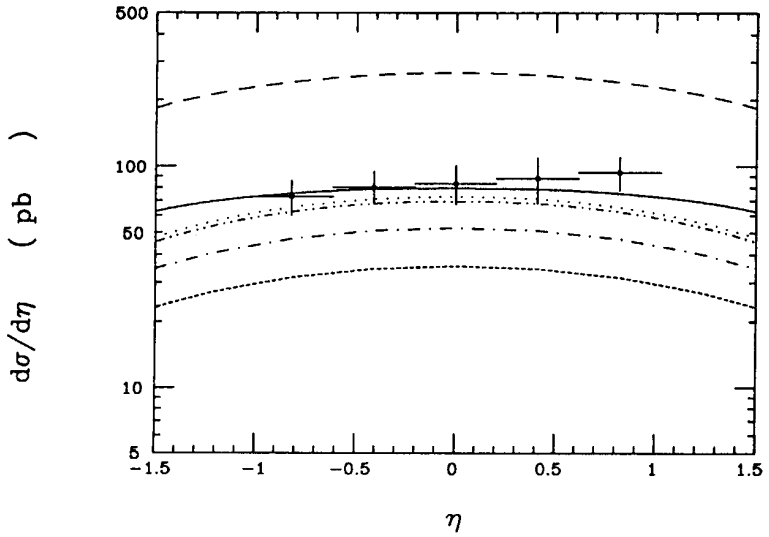

Figure 7: Inclusive jet cross sections as a function of η integrated over $|P_T| \geq 2.5$. The curves represent the sum of the QPM (direct) and MJET (resolved) cross sections using the LAC1 (full line), GRV (double-dot-dashed line), DG (dotted line), LAC3 (dashed line) and LAC1 with the gluon components excluded (dot-dashed line) parton densities. The short-dashed curve represents the QPM cross section. The plotted errors are the quadrature sums of the statistical and systematic errors.

The data are well described by LAC1, DG and GRV, but the LAC3 parameterization is excluded. Also shown in the figures are the LAC1 predictions with the contributions from the gluon density excluded. The "gluon-off" predictions for DG and GRV are similar to those for LAC1 and are not shown in the figures. It can be seen that contributions from the gluon density, which amount to nearly half of the cross section, are essential. Even though the gluon densities for these models differ significantly, the jet transverse momentum and the jet pseudo-rapidity distributions are almost the same. Thus, these general distributions are not very sensitive for distinguishing between the LAC1, DG and GRV densities. The TOPAZ group has made a similar analysis for P_T^{jet} distributions using a slightly tighter cut on the pseudo-rapidity of jets, $|\eta^{jet}| < 0.7$. The H1 experiment at HERA has measured the inclusive jet cross-sections as a function of the jet transverse energy, E_T, and the jet pseudo-rapidity, η [28]. Their E_T distribution agrees with predictions of LAC2 and GRV. However, their η distribution disagrees with the predictions of LAC2 and GRV, in particular in the negative η region. In contrast, both the P_T^{jet} and η distributions of our data agree with the predictions of LAC1 and GRV. As is clear from Fig. 1, the LAC1 and LAC2 densities are very similar.

6. Conclusions

We report on measurements of the inclusive jet and two-jet cross sections in almost-real $\gamma\gamma$ collisions at TRISTAN using the AMY detector. The data are in good agreement with leading-order QCD calculations based on either the LAC1, DG or GRV parametrizations of the parton densities in the photon. The calculation based on LAC3 disagrees with the data and we do not see the deviation that is observed in the η distribution by the H1 Experiment.

Acknowledgements

We gratefully acknowledge the help of the management and the technical staff of

TRISTAN. We would like to thank Dr. M. Drees for valuable discussions on resolved photon processes. This work has been supported by the Japan Ministry of Education, Science and Culture (Monbusho) and Society for the Promotion of Science, the U.S. Department of Energy and National Science Foundation, the Korean Science and Engineering Foundation and Ministry of Education, and the Academia Sinica of the People's Republic of China.

References

[1] S. Brodsky *et al.*, *Phys. Rev. Lett.* **41** (1978) 672; *Phys. Rev.* **D19** (1979) 1418.

[2] K. Kajantie and R. Raito, *Nucl. Phys.* **B 159** (1979) 528.

[3] M. Drees and R.M. Godbole, *Nucl. Phys.* **B339** (1990) 355.

[4] W. Bartel *et al.* (JADE), *Phys. Lett.* **B107** (1981) 163; H. Aihara *et al.* (TPC/2γ), *Phys. Rev.* **D41**; H.-J. Behrend *et al.* (CELLO), *Z. Phys.* **C51** (1991) 365.

[5] Ch. Berger *et al.* (PLUTO), *Z. Phys.* **C33** (1987) 351.

[6] R. Tanaka *et al.* (AMY), *Phys. Lett.* **B277** (1992) 215.

[7] T. Ahmed *et al.* (H1), *Phys. Lett.* **B297** (1992) 205.

[8] M. Derrick *et al.* (ZEUS), *Phys. Lett.* **B297** (1992) 404.

[9] H. Hayashii *et al.* (TOPAZ), *Phys. Lett.* **B314** (1993) 149.

[10] D. Buskuli *et al.* (ALEPH), CERN-PPE/93-94, 1993.

[11] M. Drees and R. M. Godbole, *Phys. Rev. Lett.* **67** (1991) 1189; P. Chen, *Proc. of the IXth Int. Workshop on Photon-Photon Collisions*, San Diego, California (1992) 418; M Drees, *ibid.*, 430; J.R. Forshaw and J.K. Storrow, *ibid.*, 442.

[12] T. Sjöstrand, *CERN-TH-6488-92* (May 1992) 284.

[13] T. Kumita *et al.* (AMY), *Phys.Rev.* **D42** (1990) 1339.

[14] T. Sjöstrand and H. Bengtsson, *Comp. Phys. Comm.* **43** (1987) 367.

[15] S.D. Ellis *et al.* , *Phys. Rev.* D40(1989) 2188; *Phys. Lett.* **B107** (1981) 1.

[16] J.J. Sakurai and D. Schildknecht, *Phys. Lett.* **B40** (1972) 121.

[17] M. Kuroda, *Meiji Gakuin Univ. (Tokyo) Research J.* **424** (1988) 27.

[18] Ch. Berger *et al.* (PLUTO), *Z. Phys.* **C26** (1984) 191; **C29** (1985) 499.

[19] R.D. Field and R.P. Feynman, *Nucl. Phys.* **B136** (1978) 1.

[20] S. Kawabata, *Comp. Phys. Comm.* **41** (1986) 127.

[21] To take into account the anti-tag condition, we used the luminosity function given in eq.(2.19) of Ch. Berger and W. Wagner, *Phys. Rep.* **146** (1987) 1.

[22] D.W. Duke and J.F. Owens, *Phys. Rev.* **D26** (1982) 1600; B.L. Combridge *et al.*, *Phys. Lett.* **B70** (1977) 234; M. Gluck *et al.*, *Phys. Rev* **D18** (1978) 1501.

[23] T. Sjöstrand, *Comp. Phys. Comm.* **39** (1986) 347.

[24] M. Drees and K. Grassie, *Z. Phys.* **C28** (1985) 451.

[25] A. Levy, H. Abramowics, and K. Charchula, *Phys. Lett.* **B269** (1991) 458.

[26] M. Gluck, E. Reya and A. Vogt, *Phys. Rev.* **D46** (1992) 1973.

[27] W. Bartel *et al.* (JADE), *Z. Phys.* **C33** (1986) 23.

[28] I. Abt *et al.* (H1), *DESY 93-100*, July 1993.